Synthesis and Characterization of Ag and Silica (SiO_2) Coated Ag Based Nanofluids

A thesis submitted
in partial fulfillment of the requirements for
the award of degree of

Masters of Technology
in
Materials and Metallurgical Engineering

Submitted by
Bharat Bhushan
Reg. No. 601202002

Under the supervision of
Dr. Bhupendra Kumar Chudasama
Assistant Professor
School of Physics and Materials Science

School of Physics and Materials Science
Thapar University
(Established under section 3 of UGC Act, 1956)
Patiala -147001, India

DECLARATION

I hereby declare that the work being presented in this thesis report entitled **"Synthesis and Characterization of Ag and Silica Coated Ag Based Nanofluids"** by me in partial fulfillment of the requirements of the award of degree of **Master of Technology** in **Materials Science and Engineering** from **School of Physics and Materials Science**, Thapar University, Patiala is an authentic record of my work carried out under the supervision of **Dr. B.N. Chudasama, Assistant Professor, School of Physics and Materials Science, Thapar University**. The matter presented in this report has not been submitted in any other university for the award of Masters of Technology or any other degree.

Bharat Bhushan

Reg. No. 601202002

CERTIFICATE

This is to certify that the report entitled **"Synthesis and Characterization of Ag and Silica Coated Ag Based Nanofluids"** submitted by Bharat Bhushan 601202002 is a record of candidate's own work carried out under my supervision. To the best of my knowledge, the content of this thesis does not form a basis for the award of any other degree at Thapar University, Patiala or any other university.

(Dr. Bhupendra Kumar Chudasama)
Assistant professor
School of physics and Materials science
Thapar University, Patiala

(Countersigned by)

(Dr. Kulvir Singh)
Professor& Head
School of Physics and Materials science
Thapar University, Patiala

(Dr. S.K. Mohapatra)
Dean of Academic Affairs
Thapar University, Patiala

ACKNOWLEDGEMENTS

With deep sense of gratitude, I would like to express my sincere thanks to Dr. B.N. Chudasama, *Assistant Professor School of Physics and Materials Science, Thapar University, Patiala* for his invaluable suggestion, excellent supervision, constant encouragement, thought provoking discussion and unbiased discussion in nurturing the work during the preparation of my manuscript in this research work.

I take this opportunity to express my heartfelt regards and gratitude to Mr. Kundan Lal, *Assistant Professor, Department of Mechanical Engineering, Thapar University, Patiala* for his constructive suggestion and carrying out all thermal conductivity measurements with his expert guidance.

I am grateful to Dr. Kulvir Singh, *Professor and Head, School of Physics and Materials Science, Thapar University, Patiala* and Dr. S.K. Mohapattra, *Dean of Academic Affairs, Thapar University, Patiala* for providing me with the opportunity to conduct this work and bring it out in the present form.

I would like to convey my sincere gratitude to Ms. Chandani Khurana, Ms. Parveer Kaur, Ms. Navjot Kaur, Ms. Purnima Sharma, Ms. Samita Thakur, Ms. Sakshi Gupta, Mr. Satwinder Singh, *Research Scholars, School of Physics and Materials Science, Thapar University,* Patiala for providing immense support in performing, characterizing and evaluating the thesis work.

I would also like to thank my friends (Gaganjot, Pritampal Singh Gill, Vinoth) for their kind support and encouragement.

Last but not least; I am deeply thankful to my family members for their infinite support at each and every part of my life. Above all, I express my indebtedness to the almighty for all his blessing and kindness.

Bharat Bhushan

Reg. No. 601202002

Abstract

The main objective of this thesis is to prepare stable nanofluids using Silver nanoparticles (SNPs)/water and silica coated silver nanoparticles/water system. Nanofluids have been prepared by single-step chemical reduction method starting with silver nitrate as a metal precursor. Controlled experimental conditions have been established to synthesize spherical shape SNPs. By using polyvinylpyrrolidone (PVP) as a surfactant, sterically stabilized distilled water based nanofluids is being prepared. As synthesized SNPs were coated with silica (SiO_2) to obtain silica coated silver nanoparticles based silver nanofluids. SNPs and silica coted SNPs were characterized by X-ray diffraction (XRD), UV-visible spectroscopy, Dynamics light scattering (DLS), transmission electron microscopy (TEM), Fourier transform Infrared spectroscopy (FTIR). From the X-ray analysis it is clear that nanoparticles crystallized into face centered cubic (FCC) crystal structure. The peak broadening is a clear indicative of the formation of SNPs, which was further confirmed by TEM. UV-visible study confirms the formation of SNPs. DLS study revealed the hydrodynamics size for both the sample. TEM micrograph shows that the nanoparticle are polydisperse and spherical in shape. Formation of PVP and silica shell on the surface of silver nanoparticles was confirmed by FTIR spectroscopy. Thermal conductivity of both samples was measured at room temperature and variations of thermal conductivity with temperature were measured using KD2 pro thermal property analyzer. Thermal conductivity of both the nanofluids decreases with increasing temperature. The synthesized nanofluids may find applications in industrial cooling systems.

List of Tables

Chapter 1

Chapter 4

List of figures

Chapter 3

Chapter 4

Contents

Chapter 1 Introduction

Thermal properties of fluids play an important role in various industrial processes, like wise in heating and cooling applications. The fluids that have been traditionally used for heat transfer applications have rather low thermal conductivity. Thus, there is a need to develop new types of fluids that will be more effective in terms of exchange performance. In recent years, methods have been developed to disperse small amount of nano-sized solid particles in the liquids. The resulting colloid is a multiphase material that is microscopically uniform and is termed "nanofluids".

The key building blocks of nanofluids are nanoparticles. Nanoparticles possess high surface area to volume ratio. Nano suspensions show high thermal conductivity possibly due to enhanced convection between the solid particles and liquid surfaces. Due to lower dimension, dispersed nanoparticles helps to reduce problems like particles clogging, sedimentation etc. generally faced in micro-sized particles suspensions. This extra stability and high conductivity of dispersed particles makes them highly preferable for designing heat transfer fluids and later to design lighter, high performance and variety of industrial products such as electronic circuits, computer engines and high power lasers. Nanofluids offer the development of high performance, compact and cost effective liquid cooling systems.

1.1 Conventional methods to enhance thermal conductivity and their limitations

The old technique used to increase cooling rates was to disperse millimeter or micrometer sized particles in heat transfer fluids [1]. The major problem with these suspensions was the rapid settling of these particles. Moreover, If the fluids were kept circulating to prevent particle settling, these particles would wear out pipes, pumps and bearings. Furthermore, such particles are not applicable to microsystems because they can clog microchannels. These conventional solid fluid suspensions are not practical because they require addition of a large number of particles (>10 % by volume.) resulting in significantly greater pressure drop and pumping power.

Minimizing the size and weight of cooling systems based on microchannel cooling technology is also crucial in many applications. The current designs of thermal management system have

already adopted this extended surface technology like fins. But these design leads to heavy/bulky thermal management systems, which are not suitable for microchannel cooling. Nanofluids being developed in response to these emergent needs for more efficient heat transfer fluids in many industries.

1.2 Advantages of nanofluids

Heat transfer fluids containing suspended particles of micro/millimeter sizes suffer from numerous drawbacks like erosion of the components by abrasive action, clogging in small passages, settling of particles and increased pressure drop. Thus microfluids are not suitable for heat transfer applications and the search for new heat transfer fluids is on. Nanotechnology has provided opportunities to process and produce materials in the nanometer size range that can be suspended in traditional fluids. Nanofluids are stable and have higher thermal conductivity than micro fluids. Table 1 below compares the some of the basic properties of micro fluids with nanofluids.

Table 1. 1 Comparison of micro and nanofluids

Characteristics	**Microfluids**	**Nanofluids**
Stability	Settle	Stable
Surface/ volume ratio	1	Larger than micro particles
Clog on microchannel	Yes	No
Conductivity	Low	High
Erosion	Yes	No
Pumping power	Large	Small

1.3 Properties of nanofluids components

Various metals, non-metals and metal oxide are used as solute nanoparticle. Few of them are listed in table 2.

Various fluids like water, ethylene glycol and engine oil are used as base fluids. Properties of commonly used base fluids are listed in table 3.

Table 1. 2 Materials for solute nanoparticles and their properties

Solids/liquids	Material	Thermal conductivity(W/m-K)	Density (g/cm^3)	Melting point($^{\circ}C$)
Metallic solids	Silver	429	10.490	961
	Cooper	401	8.940	1085
	Aluminum	237	2.712	660
	Gold	318	19.320	1063
Nonmetallic solids	Diamond	3300	3.513	3550
	Carbon nano tubes	3000	1.300	3652
	Silicon	140	2.330	1414
Oxides	Alumina (Al_2O_3)	48	3.950	2072

Table 1. 3 Properties of ethylene glycol and water

Molecular formula	$C_2H_6O_2$(Ethylene glycol)	H_2O(Water)
Molar mass	62.07 g/mol.	18.02 g/mol.
Appearance	Clear, colorless liquid	Colorless, transparent
Density	1.11 g/cm^3	1 g/cm^3
Freezing point	-12.9^0 C, 260 K	0°C, 273.15 K
Boiling point	197.3^0 C , 470 K	99.980°C, 373.13 K
Viscosity	1.61×10^{-2} Pa s	0.001 Pa s at 200° C
Thermal conductivity	0.253 W/m-K	0.613 W/m- K

1.4 Parameters affecting thermal conductivity of nanofluids

Many experimental studies on effective thermal conductivity of nanofluids have been done. Thermal conductivity of nanofluids depends on many factors such as particle shape and size, temperature, particles material and basefluid.

Effect of particle size and shape

Particle size and shape is an important parameter that affects thermal conductivity of nanofluids. Chopkar *et al.* [2] was first to show the nonlinear behavior of thermal conductivity with the particle size**.** He studied the effect of size of dispersed nanoparticles for $Al_{70}Cu_{30}$/ EG nanofluids by varying the size of $Al_{70}Cu_{30}$ nanoparticles in the range from 9 nm to 83 nm. Also, the results of Chon *et al.* [3] and Hong *et al*. [4] support this conclusion drawn by chopakar. Most recently, Kim *et al*. [5] showed that the thermal conductivity of nanofluids increases linearly with decrease in particle size. The reason behind such behavior is the increase in specific surface area with the decrease in particle size. Spherical and cylindrical nanoparticles are frequently used. Cylindrical nanoparticles have larger aspect ratio than spherical nanoparticles. The wide differences in the dimensions of these particles influence the enhancement in the thermal properties of nanofluids [6]. However the cylindrical nanoparticles suspensions need higher pumping power due to its enhanced viscosity, which limits their possible applications as heat transfer fluids [7].

Effect of temperature

Most of the studies have demonstrated the temperature dependency of nanofluids. However, there is considerable disagreement in the literature regarding the temperature dependence of their thermal conductivities. According to some research groups, the thermal conductivity of nanofluid show enhancement with respect to temperature. For example Das *et al.* [8] demonstrated enhancement of the thermal conductivities of water based Al_2O_3 and CuO nanofluids. Patel *et al*. [9] reported the effective thermal conductivity of Au nanofluid enhances with increase in temperature. But other research group showed the independent of thermal conductivities with the increase in temperature. Venerus *et al*. [10] prepared Au/water nanofluids and showed thermal conductivity is independent of temperature.

Effect of particle materials

Particle material is an important parameter that affects the thermal conductivity of nanofluids. Yu *et al.* [11] considered the thermal conductivity of nanofluids with Al_2O_3 and CuO nanoparticles and they found that nanofluids with CuO nanoparticles showed better

enhancement when compared to the nanofluids prepared using Al_2O_3 nanoparticles. It should be noted that Al_2O_3 as a material has higher thermal conductivity than CuO.

Effect of base fluid

According to the conventional thermal conductivity models such as the Maxwell's model, as the base fluid thermal conductivity of a mixture decreases the thermal conductivity ratio (thermal conductivity of nanofluid/thermal conductivity of base fluid) increases. Wang *et al*. [12] prepared Al_2O_3 and CuO nanoparticles based nanofluids with several base fluids such as water, ethylene glycol, vacuum pump fluid and engine oil. With Al_2O_3 nanoparticles, the highest thermal conductivity ratio was observed when ethylene glycol was used as the base fluid. Engine oil showed somewhat lower thermal conductivity ratios than ethylene glycol.

1.5 Applications of nanofluids

Transportation

Ethylene glycol and water mixture universally used automotive coolant, is a relatively poor heat transfer fluid. The addition of nanoparticles to the standard engine coolant has the potential to improve automotive and heavy-duty engine cooling rates. Such an improvement can be used to remove engine heat with a smaller coolant system. Tzeng *et al.* [13] dispersed CuO and Al_2O_3 nanoparticles into engine transmission oil. The results showed that CuO nanofluids produced the lowest transmission temperatures both at high and low rotating speeds. Thus, the use of nanofluids in the transmission has a clear advantage from the thermal performance viewpoint.

Friction Reduction

Advanced lubricants can improve productivity through energy saving and reliability of engineered systems. Tribological research heavily emphasizes reducing friction and wear. Nanoparticles have attracted much interest in recent years due to their excellent load carrying capacity, good extreme pressure and friction reducing properties. Zhou *et al.* [14] evaluated the tribological behavior of Cu nanoparticles in oil on a four-ball machine. The results showed that Cu nanoparticles as an oil additive had better friction-reduction and antiwear properties than zinc dithiophosphate, especially at high applied load.

Cooling of microchips

Nanofluids have been considered as the working fluid for heat pipes in electronic cooling applications. Tsai *et al.* [15] used water-based nanofluid as the working medium in a circular heat pipe designed as a heat spreader to be used in a CPU in a notebook or a desktop PC. The results showed a significant reduction in thermal resistance of the heat pipe with the nanofluid as compared to deionized water. The measured results also showed that the thermal resistance of a vertical meshed heat pipe varies with the size of nanoparticles. Jang *et al.* [16] designed a cooler, combined microchannel heat sink with nanofluids. Higher cooling performance was obtained when compared to the device using pure water as working medium. Nanofluids reduced both the thermal resistance and the temperature difference between the heated microchannel wall and the coolant.

Microscale Fluidic Applications

The manipulation of small volumes of liquid is necessary in fluidic digital display devices, optical devices and microelectromechanical systems (MEMS) such as lab-on-chip analysis systems. This can be done by electro wetting or by reducing the contact angle by an applied voltage, the small volumes of liquid. Electro wetting on dielectric (EWOD) actuation is very useful method of microscale liquid manipulation. Vafaei *et al.* [17] showed that addition of very low concentration bismuth telluride nanofluids dramatically changes the wetting characteristics of surface. This potential wetting characteristics of nanofluids can be used to move liquid efficiently in microsystems.

Energy Storage

The storage of thermal energy in the form of sensible and latent heat has become an important aspect of energy management with the emphasis on efficient use and conservation of the waste heat and solar energy in industry and buildings [18]. Latent heat storage is one of the most efficient ways of storing thermal energy. Wu *et al.* [19] evaluated the potential of Al_2O_3/H_2O nanofluids as a new phase change material (PCM) for the thermal energy storage of cooling systems. The thermal response test showed the addition of Al_2O_3 nanoparticles remarkably decreased the supercoiling degree of water, advanced the beginning freezing time, and reduced

the total freezing time. Only adding 0.2 wt. % Al_2O_3 nanoparticles, the total freezing time of Al_2O_3/H_2O nanofluids could be reduced by 20.5%.

Solar Absorption

Solar energy is one of the best sources of renewable energy with minimal environmental pollution. The conventional direct absorption solar collector is a well-established technology, and it has been proposed for a variety of applications such as water heating; however, the efficiency of these collectors is limited by the absorption properties of the working fluid, which is very poor for typical fluids used in solar collectors. Recently, this technology has been combined with the emerging technologies of nanofluids and liquid-nanoparticle suspensions to create a new class of nanofluid-based solar collectors. Otanicar *et al.* [20] reported the experimental results on solar collectors based on nanofluids made from a variety of nanoparticles. The efficiency improvement was up to 5 % in solar thermal collectors by utilizing nanofluids as the absorption media.

Intensify Microreactors

High enhancement of heat transfer in nanofluids can be applicable to the area of process intensification of chemical reactors. Fan *et al.* [21] studied a nanofluid based on benign TiO_2 material dispersed in ethylene glycol in an integrated reactor heat exchanger. The overall heat transfer coefficient increase was up to 35% in the steady state continuous experiments. This resulted in a closer temperature control in the reaction of selective reduction of an aromatic aldehyde by molecular hydrogen and very rapid change in the temperature of reaction under dynamic reaction control.

Chapter 2 Literature Review

Various studies on nanofluids were carried out by researchers in the past. This chapter reviews the literature, which lays foundation and basis for this work. This helps us to give a better understanding about the topic and also acts as a guideline for our thesis. In this chapter, experimental and theoretical efforts on synthesis process, characterization of nanofluids and detailed proposed theories for explaining the experimental results have been reviewed and discussed**.** Choi *et al.* [22] first prepared nanofluids by mixing nanoparticles with fluid. Since then, there has been a rapid development in the synthesis techniques for nanofluids.

S.U. S. Choi *et al.* [22] proposed the innovative new class of heat transfer fluids that can be engineered by suspending metallic nanoparticles in conventional heat transfer fluids. Theoretical study for the thermal conductivity of nanofluids with copper nano phase materials were presented and the potential benefits of the fluids were estimated. It is shown that one of the benefits of nanofluids will be dramatic reductions in the power of heat exchanger pump.

S. Lee *et al.* [23] prepared oxide nanofluids of Al_2O_3 and CuO as dispersion. Thermal conductivity was measured by transient hot-wire method. The results showed that these nanofluids, containing a small amount of nanoparticles have higher thermal conductivity than same liquid without nanoparticles. Comparisons between experiments and the Hamilton and Crosser model showed that the model can predict the thermal conductivity of nanofluids containing Al_2O_3 particles but inadequate for nanofluids containing CuO particles. This showed that not only particle shape but size is considered to be dominant in enhancing the thermal conductivity of nanofluids.

G. Carotenuto [24] prepared silver nanoparticles in ethylene glycol by the reduction of $AgNO_3$ in the presence PVP as a reducing agent. The reaction was carried out at room temperature and the process of particle growth was terminated by acetone addition. Characterization of the nanocomposite prepared by above method showed that silver clusters with a uniform size distribution were obtained. A more uniform distribution could be obtained by increasing the temperature. However, in this case the reaction rate is high and the particle growth process is difficult to stop at the cluster level.

P. Keblinsi *et al.* [25] showed that thermal conductivity increases with decreasing size of suspended nanoparticles. Four mechanisms were proposed: Brownian motion of the particles, molecular level layering of liquid at the liquid/particle interface, the nature of heat transport in nanoparticles and effect of nanoparticles clustering. Moreover, they showed that the key factor in understanding the thermal properties of nanofluids is ballistic, rather than diffusive nature of heat transport.

S. K. Das *et al.* [26] investigated the increase of thermal conductivity with temperature for nano fluids with water as base fluid and particles of Al_2O_3 or CuO as suspension material. A temperature oscillation technique was used for the measurement of thermal diffusivity and thermal conductivity. The results indicate an increase in enhancement characteristics with temperature, which makes the nanofluids even more attractive for applications with high energy density than usual room temperature measurements reported earlier.

H. Wang *et al.* [27] reported the synthesis of silver nanoparticles by glucose in the presence of polyvinyl pyrrolidone (PVP). Sodium hydroxide was used to enhance the reaction rate. The mole ratio of NaOH to $AgNO_3$ was changed from 1.4 to 1.6. The particles and colloids were analyzed by the X-ray diffraction (XRD), transmission electron microscopy (TEM) and UV–Visible spectroscopy. The results indicated that with the increase in PVP, the particles dispersed better and with the weight ratio of PVP to $AgNO_3$ no less than 1.5, the particles dispersed individually in a colloidal form. The speed of the reactants mixing also influenced the agglomeration of nanoparticles.

T. Cho *et al.* [28] prepared silver nanofluids by chemical reduction method using silver nitrate (precursor), ethylene glycol (reducing agent), poly (acryl-amide-*co*-acrylic acid) (dispersion stabilizer). For different amount of dispersion stabilizer, size and distribution were investigated. Thermal conductivity of samples with different concentrations of silver was investigated. The samples were characterized with UV-Visible spectrophotometer and TEM. Thermal conductivity was analyzed with KD-2 pro. An enhancement of 10%, 16% and 18% with particle concentration of 1000, 5000 and 10000 were reported.

D. Kim *et al.* [29] synthesized spherical silver nanoparticles with various sizes by the polyol process. Two different synthesis methods were compared in order to investigate the influence of reaction parameters on the resulting particle size and its distribution. In the precursor heating method, wherein a solution containing silver nitrate was heated to the reaction temperature, the ramping rate was determined to be a critical parameter affecting the particle size. In contrast, in the precursor injection method, in which a silver nitrate aqueous solution was injected into hot ethylene glycol, because of rapid nucleation, the injection rate and the reaction temperature were important factors in terms of reducing the particle size and attaining monodispersity. Silver nanoparticles with a size of 17 ± 2 nm were obtained at an injection rate of 2.5 mL s^{-1} and a reaction temperature of 100°C.

J. S. Kim [30] prepared silver nanoparticles by reduction of $AgNO_3$ in ethanol in the presence of polymer (PVP) as a protective agent. UV-visible spectrum showed a strong plasmon resonance at 402 nm. The band position depends on PVP: $AgNO_3$ weight ratio of silver colloids. The rate constant depends on the PVP: $AgNO_3$ weight ratio and reaction temperature.

M. A. S. Sadjadi *et al.* [31] synthesized silver nanorods with average length of 280 nm and around diameter of about 25 nm by chemical reduction method in the presence of polyvinylalcohol (PVA). The samples were investigated by SEM, XRD, TEM and UV-Visible spectroscopy. It was found that both temperature and reaction rates plays an important role in controlling morphology and aspect ratio of nanorods.

S. G. Kim *et al.* [32] synthesized silica-coated Ag nanoparticles using water-soluble micelle under basic condition. Monodispersed Ag nanoparticles were obtained in the presence of ascorbic acid with mean particle size of 7 nm. A silica layer was adsorbed on the surface of Ag nanoparticles by using tetraethyl orthosilicate (TEOS) as precursor. Controlled experimental parameters like concentrations of surfactant, Ag nanoparticles and TEOS resulted in formation of nanoparticles size from 50-100 nm. Nanoparticles were characterized by UV-visible spectrophotometer, TEM and XRD.

J. E. Millstone *et al.* [33] has reported various photochemical and thermal methods to prepare silver and gold nano triangular prism. In addition, they developed thermal synthesis to

produce high yield of nanoparticles and to control the formation of gold and silver nano prism. These processes helped to better understand the formation of anisotropic nanostructure from metal ion precursors. It is also necessary to study both crystallographic and redox reaction to understand the overall mechanism.

H. A. Mintsa *et al.* [34] reported effective thermal conductivity of Al_2O_3/water and Cu/water nanofluids. The effects of particle volume fraction, temperature and particle size were investigated. Thermal conductivity measurement was taken in the range of 20-40˚C for various particle volume fractions up to 9%. Results showed that an increase in the effective thermal conductivity with an increase in particle volume fraction, decreased in particle size. Obtained results were comparable with certain data sets and theoretical models found in literature.

M. Chandrasekar *et al.* [35] reported the experimental investigations and theoretical determination about the effective thermal conductivity and viscosity of Al_2O_3/H_2O nanofluid. The nanofluid was prepared by synthesizing Al_2O_3 nanoparticles using microwave assisted chemical precipitation method, nanoparticles were then dispersed in distilled water by sonication. Al_2O_3/water nanofluid with a nominal diameter of 43 nm at different volume concentrations (0.33–5%) at room temperature were used for the investigation. The thermal conductivity and viscosity of nanofluids were measured .The results showed that the viscosity increase is substantially higher than the increase in thermal conductivity for nanofluids. Both the thermal conductivity and viscosity of nanofluids increase with the nanoparticle volume concentration. Maxwell and Einstein models showed reasonably good agreement with experimental results.

J. G. Barrasa *et al.* [36] used chemical reduction methods to synthesize silver nanoparticles by taking different precursors and reducing agents and also different silver nanostructured synthesized through the reduction of silver nitrate in ethylene glycol in the presence of PVP like nano sphere, nano rods, nano cubes and nanowires.

M. Chandrasekar *et al.* [37] reported the possible mechanism that contributed to enhanced thermal conductivity of nanofluids. The other factors affecting the nanofluids thermal conductivity discussed. The mathematical models for estimating nanofluids thermal conductivity

with their limitations were also developed. They concluded that there is big gap existing between the experimental data and theoretical predictions.

E. P. J. Sudhan *et al.* [38] reported the synthesis of silver nanofluid by a novel one-pot method. Silver nanofluid was prepared by reducing silver nitrate in the presence of sodium hypophosphite as a reducing agent and sodium lauryl sulphate (SLS) as surfactant. Effect of concentration of silver nitrate, SLS on the size of the nanoparticle and pH on time of synthesis of silver nanofluid was studied. The characterization of silver nanofluid was done by means of particle size analyzer. The heat transfer efficiency of the nanoparticles was evaluated by transient hot wire method.

C. Pang *et al.* [39] prepared methanol-based nanofluids with Al_2O_3 and SiO_2 nanoparticles using ultrasonic equipment. Thermal conductivity, zeta potential, particle size and Tyndall effect were studied. The transient hot-wire method was applied for measuring the thermal conductivity of methanol-based nanofluids. The results showed that the thermal conductivity increases with an increase of the nanoparticle volume fraction and the enhancement were 10.74% and 14.29% over the basefluid at the volume fraction of 0.5 % for Al_2O_3 and SiO_2 nanoparticles, respectively. Clustering of nanoparticles is considered to be the main reason for the thermal conductivity enhancement.

R. S. Khedkar *et al.* [40] Effect of CuO nanoparticles on the thermal conductivity of base fluids like mono ethylene glycol and water was studied. Both the basefluids showed enhancement in effective thermal conductivity with the addition of CuO nanoparticles. This enhancement was investigated with regard to various factors: concentration of nanoparticles, types of base fluids and sonication time. In both the base fluids, an improvement in thermal conductivity was found as concentration of nanoparticles increased due to interaction between nanoparticles. It was also found that as the sonication time was increased, there was further more improvement in the thermal conductivity of the base fluids.

Chandni *et al.* [41] reported the growth kinetics of ultrafine monodispersed silver nanoparticles prepared by thermal reduction of silver nitrate in the presence of oleylamine. Effect on nucleation and growth temperature and time on the quantity and quality of silver

nanoparticles was studied through product yield, crystal phase, morphology, aggregation, particle size and distribution. UV-Vis spectroscopy, XRD, TEM, FTIR, photon correlation spectroscopy were performed to characterize silver nanoparticles and to understand the effect of growth kinetics of reaction.

J. M. Salehi *et al.* [42] has reported the one step method for the preparation of stable and non-agglomerated silver nanofluids. Silver nanoparticles were prepared by reducing silver nitrate in the presence of sodium borohydride and hydrazine as reducing agents and polyvinylpyrrolidone (PVP) as surfactant. Distilled water was used as a base fluid. The characterization of the nanofluid were done by particle size analyzer, X-ray diffraction topography, UV-visible absorption spectroscopy and transmission electron microscopy followed by the study of thermal conductivity of nanofluid by the transient hot wire method. The results showed that Ag-water nanofluids with low concentration of nanoparticles, i.e., below 1000 ppm, have noticeably higher thermal conductivities than the water base fluid without Ag. Moreover, the amount of PVP in silver nanofluid can have a significant effect on magnitude and behavior of the thermal conductivity enhancement.

X. Fang *et al.* [43] studied the effect of adding silver (Ag) nanoparticles of various shapes on the thermal conductivity enhancement of ethylene glycol (EG)-based suspension. Three different shaped Ag (nanowires, nano sphere and nano flakes) nanoparticles were studied. Thermal conductivity of these different nanofluids was measured in the temperature range of 10˚-30˚C. Out of all these nanoparticles, nanowires with high aspect ratio (~500) showed highest increase in thermal conductivity.

Chapter 3 Experimental Techniques

This chapter outlines the synthesis procedure and basic theories and principles for various experimental techniques like UV-Visible spectroscopy, Dynamics Light Scattering (DLS), X-ray Diffraction (XRD), Fourier Transform Infra-Red spectroscopy (FTIR), Transmission Electron Microscopy (TEM) and KD2Pro Thermal properties analyzer.

3.1 Synthesis of nanofluids

Nanofluids are prepared by dispersing nanometer- sized solid particles into liquids such as water, ethylene glycol or oils. Modern fabrication techniques provide great opportunities to process materials at nanometer scales. There are mainly two techniques for synthesizing nanofluids [44]:

(a) Two-step method

(b) Single-step method

(a) Two-step method

Two-step method is the most widely used method for preparing nanofluids. In this method, nanoparticles are first prepared separately as dry powders by chemical or physical methods typically by inert gas condensation. Then, the nanosized powder is dispersed into a fluid with the help of magnetic stirring, ultrasonic agitation, high-shear mixing, homogenizing and ball milling. Two-step method is the most economic method to produce nanofluids in large scale because nanopowders synthesis techniques have already been scaled up to industrial production levels. Drawback of this method is the tendency of nanoparticles to agglomerate during the storage and dispersion in the base fluids, particularly with heavier metallic nanoparticles. Stability or nanoparticles in fluids can be increased by use of surfactant. Due to difficulty in preparing stable nanofluids by two-step method, several advanced techniques are developed to prepare nanofluids like one-step method.

(b) One-step method

The one-step process consists of simultaneously making and dispersing nanoparticles in the fluid. In this method, the processes of drying, storage, transportation and dispersion of

nanoparticles are avoided, so the agglomeration of nanoparticles is minimized and the stability of fluids increases [45]. The one-step processes can prepare uniform nanoparticles which are well dispersed in the base fluids. To reduce the agglomeration of nanoparticles, Eastman et al. have developed a one-step physical vapor condensation method to prepare Cu/ethylene glycol nanofluids [46].

Zhu et al. [47] presented a novel one-step chemical method for preparing copper nanofluids by reducing $CuSO_4 \cdot 5H_2O$ with $NaH_2PO_2 \cdot H_2O$ in ethylene glycol under microwave irradiation. Well-dispersed and finely suspended copper nanofluids were obtained. Stable ethanol-based nanofluids containing silver nanoparticles were prepared by one-step method [48]. Polyvinylpyrrolidone (PVP) was employed as the stabilizer and reducing agent for silver in solution.

In the present report, synthesis of silver nanofluids and silica coated silver nanofluids was carried out by one step method. Both samples were characterized by UV-Visible spectroscopy, Dynamics Light Scattering (DLS), Fourier transform infrared spectroscopy (FTIR), X-ray diffraction (XRD) and Transmission electron microscopy (TEM). Thermal conductivity of both the samples was measured with KD2 Pro thermal property analyzer.

3.2 Materials

Silver nitrate ($AgNO_3$) (99.9%) was procured from S.D. fine-chem. India Ltd. Ethylene glycol (99.8%), Polyvinylpyrrolidone (PVP10) and tetraethyl orthosilicate (TEOS) were purchased from Sigma-Aldrich. Ammonia solution (25%) was purchased from Loba chemicals. Synthesis was carried out in ultrapure Milli Q (specific resistance of 18.2 MΩ/cm) water. All the chemicals were used as-received without any further purification.

3.3 Synthesis of Silver Nanofluid

Synthesis of silver nanoparticles (SNPs) was carried out by a simple one pot method. SNPs were formed by reducing $AgNO_3$ with PVP. It acts as both reducing and capping agent. Furthermore PVP plays an important role in controlling the size and shape of metal nanoparticles. The hydrophilic amide group of PVP is bound to the surface of metal nano particles due to strong affinity of N and O atom for transition metal, whereas polyvinyl part of PVP forms a

hydrophobic domain, which surrounds the metal particles and protects them from agglomeration [46].

A solution containing 100 mL ethylene glycol and 0.75 mM PVP were prepared in a 250 mL beaker. This Solution was heated and stirred @ 160˚ C for 1 hour. To this solution, a mixture of 1.5 mM silver nitrate ($AgNO_3$) and 5 mL ethylene glycol were added. The solution was again heated and stirred @ 160 ˚C for 2 hour. This results in the formation of SNPs. Resulting solution was then cooled to room temperature. After this, the solution was centrifuged three times with ethanol @12000 rpm for 10 min. SNPs were re-dispersed in distilled water, to obtain silver nanofluid. Flow chart for synthesis protocol used above is shown in fig. 3.1

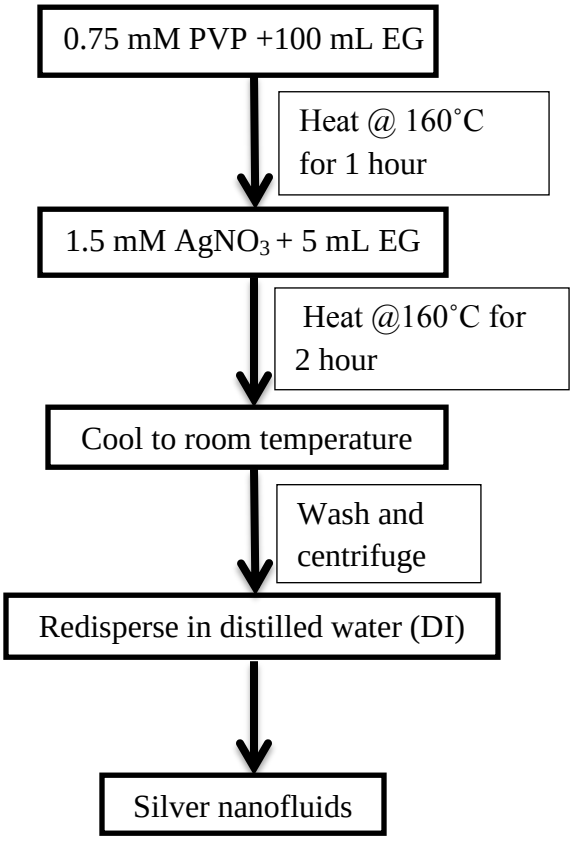

Fig. 3. 1: Flow chart for synthesis of silver nanofluids

3.4 Silica coated Silver Nanofluid

3.4.1 Hydrolysis and Condensation

Hydrolysis is a chemical process in which a molecule of water is added to a substance. Sometimes this addition causes both substance and water molecule to split into two parts. In such reactions, one fragment of the target molecule (or parent molecule) gains a hydrogen ion. A condensation reaction, also commonly referred to as dehydration synthesis is a chemical reaction in which two molecules or moieties (functional groups) combine to form a larger molecule, together with the loss of a small molecule. Possible small molecules lost are water, hydrogen chloride and methanol. Hydrolysis and condensation reaction are shown in fig.3.2

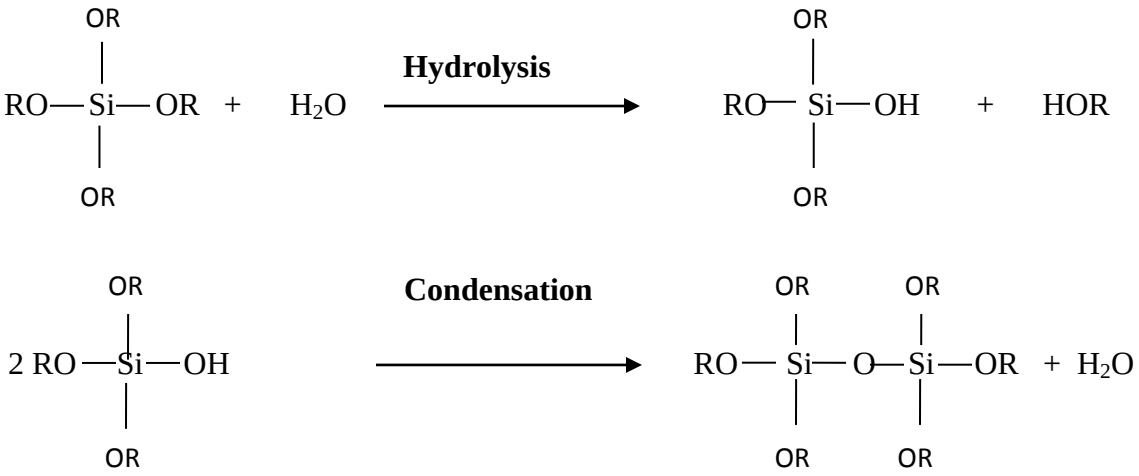

Fig. 3. 2: Hydrolysis and condensation alkoxysilanes

3.4.2 Synthesis

A solution of 100 mL ethanol, 335 mL distilled water, 20 mL ammonia and 0.165 mL TEOS was added in a beaker. To this, a colloidal solution of SNPs prepared earlier was added and then mechanically stirred for 1 hour at room temperature. This results in coating of SNPs by silica shell. SNPs coated with silica were centrifuged and washed 5 times with ethanol followed by a distilled water wash to remove impurities. The precipitates were re-dispersed in distilled water and this prepares silica coated silver nanofluids.

3.4.3 Kinetics of hydrolysis and condensation of TEOS

As synthesized silver nanofluid were coated with silica (SiO_2) by hydrolysis and condensation of Tetraethyl orthosilicate (TEOS) by chemical route. Ammonium hydroxide was used as catalyst. Adsorbed surfactant layers (PVP) on the surface of Ag nanoparticles were used as templates for silica coating due to hydrophobic nature of TEOS [49]. The addition of TEOS in the mixture of ethanol–water begins the hydrolysis and condensation of TEOS. Under the basic condition, water dissociates to produce nuleophilic hydroxyl anion (OH^-) and then hydroxyl anion attaches the silicon atom.

Hydrolysis reaction

$$Si(OC_2H_5)_4 + H_2O \longrightarrow Si(OC_2H_5)(OH) + C_2H_5OH$$

Condensation reaction

$$Si\text{-}OC_2H_5 + HO\text{-}Si \longrightarrow Si\text{-}O\text{-}Si + C_2H_5OH \text{ (Alcoholic condensation)}$$

$$Si\text{-}OH + HO\text{-}Si \longrightarrow Si\text{-}O\text{-}Si + H_2O \text{ (water condensation)}$$

Overall reaction

$$Si(OC_2H_5)_4 + 2H_2O \longrightarrow SiO_2 + 4C_2H_5OH$$

In condensation reaction, the intermediate Si-OH condenses to form embryos of silica (SiO_2). The condensation of $Si(OH)_4$ will nucleate embryos of silica. These embryos are colloidally unstable and readily aggregate to form larger particles. This silica will chemically adsorb on the surface of PVP capped Ag nanoparticles.

3.5 Characterization techniques

3.5.1 UV-Vis-spectroscopy

UV-Vis-spectrophotometer is analytical technique that uses light in visible, ultraviolet and near infrared ranges. UV-Vis spectroscopy refers to absorption spectroscopy in the ultraviolet-visible spectral region. In this region of electromagnetic spectrum, molecules undergo electronic

transitions. The absorption of light occurs very quickly in femto-seconds. The energy in quantum is expressed by equation:

$$\mathbf{E=h\nu=hc/\lambda}$$

Where E is the energy, h is the Planck's constant, ν and λ are the frequency and wavelength of the incoming photon and c is the velocity of light. Absorption of visible and ultraviolet radiations is associated with excitation of electron in both atoms and molecules to higher energy states. All molecules will undergo electronic excitation following adsorption of light but for most molecules very high energy radiation (in the vacuum ultraviolet < 200nm) is required. For molecules containing conjugated electron systems however, light in the UV-Visible region is adequate.

Principle of operation:

A beam of light from a visible and/or UV light source is separated into its component wavelengths by a prism or diffraction grating. Each monochromatic beam in turn is split into two equal intensity beams by partially silvered mirrors as shown in fig.3.3. The sample beam passes through a small transparent container (cuvette) containing a solution of the compound being studied in a transparent solvent. The reference passes through an identical cuvette containing only the solvent. The intensities of these light beams are then measured by electronic detectors and compared. The intensity of reference beam which should have suffered little or no light absorption is I_0.The intensity of sample beam is I. Over a short period of time, the spectrometer automatically scans all the components wavelengths in the UV region (200-400nm) and visible region (400-800nm).

The Beer-Lambert law states that absorbance of a solution is directly proportional to the concentration of the absorbing species in the solution and the path length. Thus, for a fixed path length, UV/Vis spectroscopy can be used to determine the concentration of the absorber in the solution. The amount of light I, transmitted through the solution of an absorbing chemical in a transparent solvent can be related to its concentration by Beer Laws:

$$\mathbf{-Log\ I/I_0 = A = \epsilon \times b \times c}$$

Where I_o is the incident light intensity, A is the absorbance, b is the cell Path length in cm, c is the solution concentration in moles/liters, ϵ is the molar absorptivity (also referred to as the molar extiction coefficient) which has units of litre $mole^{-1}cm^{-1}$.

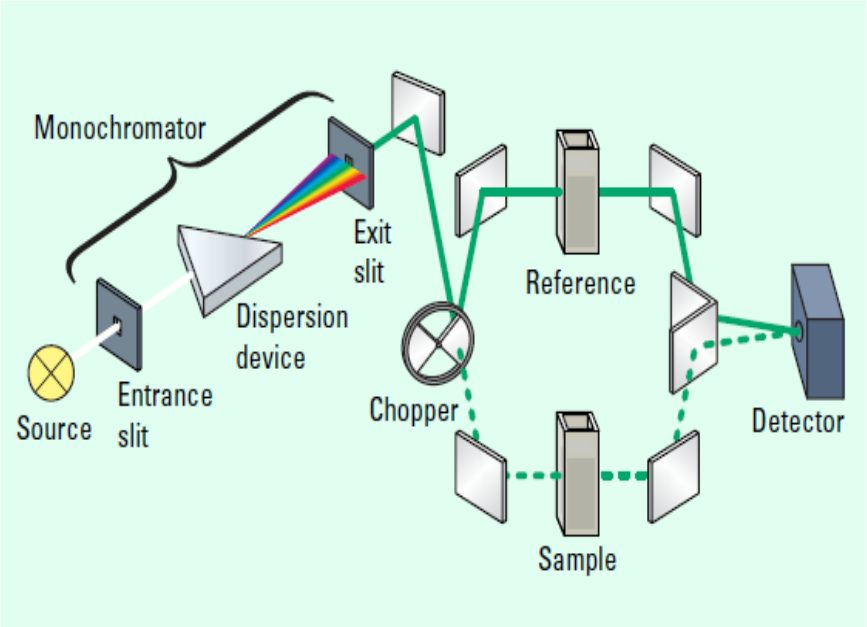

.

Fig. 3. 3: Schematic of UV-Visible spectrophotometer

3.5.2 Fourier Transform Infrared Spectroscopy (FTIR)

FTIR spectroscopy is used primarily for qualitative and quantitative analysis of organic compounds and also for determining the chemical structure of many inorganic compounds. FTIR is a technique which is used to obtain an infrared spectrum of absorption, emission, photoconductivity or Raman scattering of a solid, liquid or gas. FTIR spectrometer simultaneously collects spectral data in a wide spectral range. This confers significant advantages over a dispersive spectrometer which measures intensity over a narrow range of wavelength at a time. An FTIR technique has made dispersive infrared spectrometers all but obsolete. The FTIR originates from the fact that a Fourier transforms (a mathematical algorithm) is required to convert the raw data into the actual spectrum. The main goal of IR spectroscopy is to determine the chemical functional group in the sample. Different functional group absorb at characteristic frequencies.

Principle of operation

Chemical bonds absorb infrared energy at specific frequencies (or wavelength), the basic structure of compounds can be determined by the spectral locations of their IR absorptions. The plot of a compound's IR spectra is its "fingerprint", which when compared to the reference spectra identifies the material.

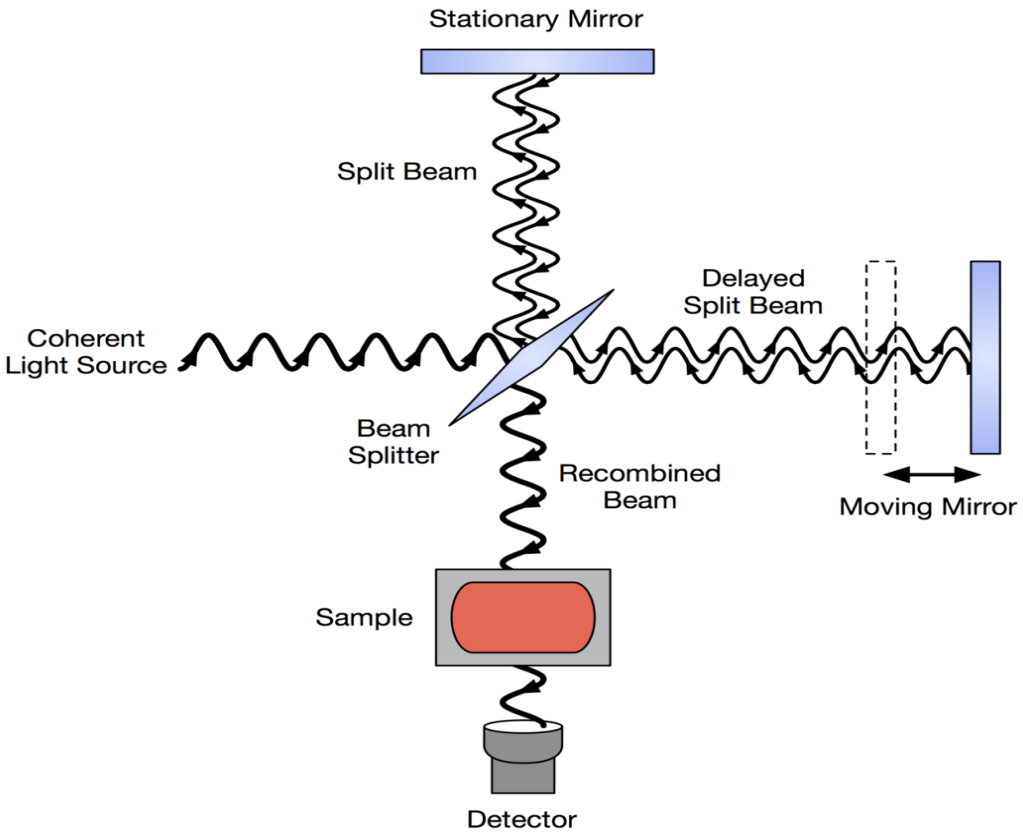

Fig. 3. 4: Schematic of FTIR spectrophotometer

An FTIR is typically based on a Michelson interferometer. The interferometer consists of a beam splitter, a fixed mirror and a mirror that translates back and forth very precisely as shown in fig. 3.4. The beam splitter is made of a special material that transmits half of the radiation striking it and reflects the other half. Radiation from the source strikes the beam splitter and separates it into two beams. One beam is transmitted through the beam splitter to the fixed mirror and the second is reflected off the beam splitter to the moving mirror. The fixed and moving mirrors reflect the radiation back to the splitter. Again, half of this reflected radiation is transmitted and

half is reflected at the beam splitter, resulting in one beam passing to the detector and the second back to the source.

3.5.3 Dynamic Light Scattering (DLS)

Dynamic Light Scattering (also referred to as Photon Correlation Spectroscopy or Quasi-Elastic Light Scattering) is a technique for measuring the size of particles typically in the sub-micron region. DLS measures Brownian motion and relates this to the size of the particles. Brownian motion is the random movement of particles due to the bombardment by the solvent molecules that surround them. Normally DLS is concerned with measurement of particles suspended within a liquid. The larger the particle, the slower the Brownian motion will be. Smaller particles are "kicked" further by the solvent molecules and move more rapidly. Brownian motion is defined by a property known as the translational diffusion coefficient (D).

The hydrodynamics size of a particle is calculated from the translational diffusion coefficient by using the Stokes- Einstein equation;

$$d(\mathrm{H}) = \frac{kT}{3\pi\eta D}$$

Where *d(H)* = hydrodynamic diameter, D = translational diffusion coefficient, *k* = Boltzmann's constant, *T* = absolute temperature and η = viscosity. The diameter that is obtained by this technique is the diameter of a sphere that has the same translational diffusion coefficient as the particle. The translational diffusion coefficient will depend not only on the size of the particle "core", but also on the surface structure, as well as the concentration and type of ions in the medium.

Working

In dynamic light scattering, the speed at which the particles are diffusing due to Brownian motion is measured. This is done by measuring the rate at which the intensity of the scattered light fluctuates when detected using a suitable optical arrangement. The schematic of light scattering by small and large particles is shown in fig. 3.5.

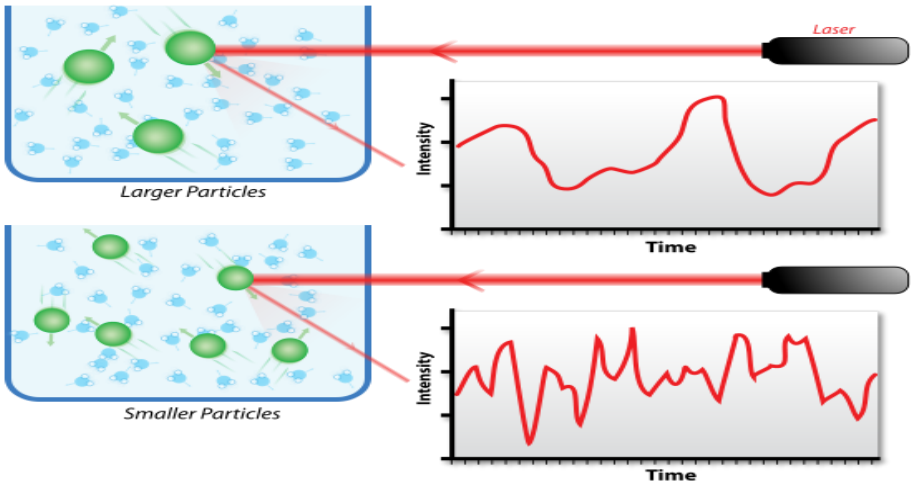

Fig. 3. 5: Schematic of scattering by small and large particles

3.5.4 X-ray diffraction (XRD)

The extensive use of X-rays for the analysis of atomic structural arrangements is based on the fact that waves undergo a phenomenon called diffraction when interacting with systems which are spaced at distances of the same order of magnitude as the wavelength of the particular radiation considered. X-ray diffraction in crystalline solids takes place because the atomic spacing is in the 10^{-10} m range, comparable to X-rays. Schematic of X-ray diffraction is shown in fig. 3.6.

The atomic structure of crystalline solids is commonly determined using one of several different X-ray diffraction techniques. Complementary structure information can also be obtained through electron and neutron diffraction. In all instances, the radiation used must have wavelengths in the range of 0.1 to 10 Å because the resolution (or smallest object separation distance) to which any radiation can yield useful information is equal to the wavelength of the radiation and the average distance between adjacent atoms in solids is about 10^{-10}m (1 Å). Since there is no convenient way to focus X-rays with lenses and to magnify images, we do not attempt to look directly at atoms. Rather, we consider the interference effects of X-rays when scattered by the atoms, comprising a crystal lattice. This is analogous to studying the structure of an optical diffraction grating by examining the interference pattern produced when we shine visible light on the grating. In the optical grating the ruled lines act as scattering centers, whereas in a crystal it is the atoms (more correctly, the electrons about the atom) which scatter the incident

radiation. The geometrical conditions which must be satisfied for diffraction to occur in a crystal were first established by Bragg's law.

$$n\lambda = 2\, d\sin\theta$$

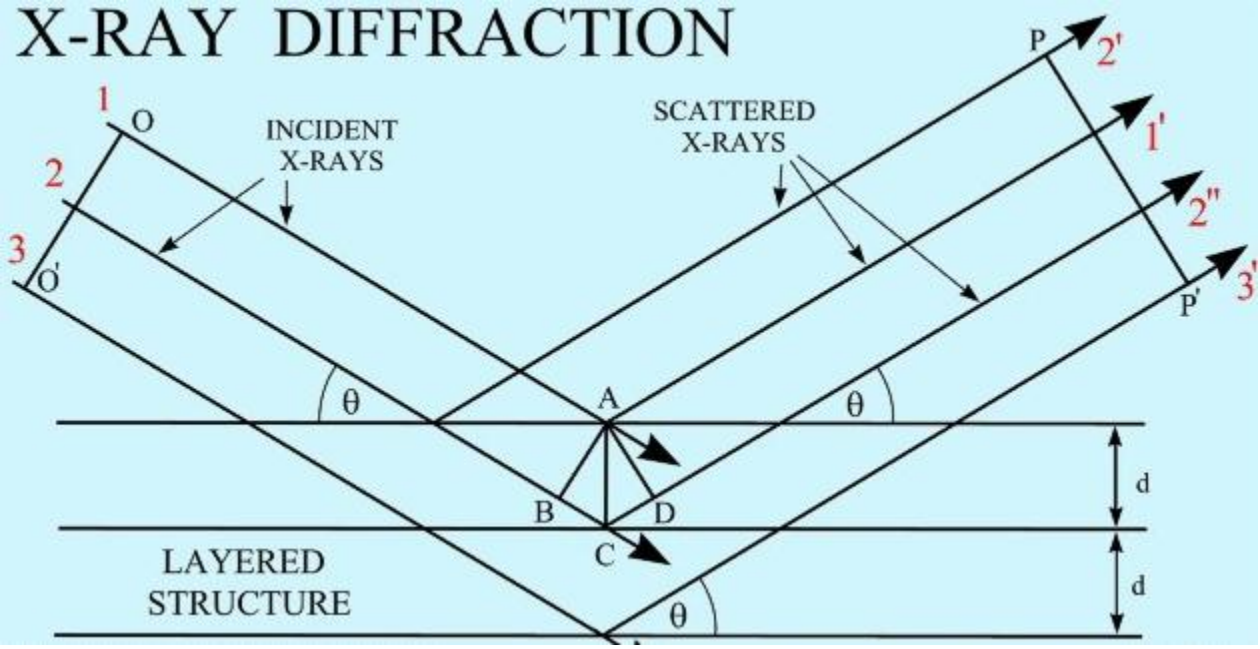

Fig. 3. 6: Schematic of X-ray diffraction

The rays which satisfy the Bragg's law undergoes constructive interference hence sharp peak is observed corresponding to that angle. These peaks are collected by detector and plot of intensity versus 2θ is generated.

Applications

1. Degree of crystallinity.
2. Crystalline phase and crystal structure.
3. Crystallite size from analysis of peak broadening.

3.5.5 Transmission electron microscopy (TEM)

TEMs were developed because of the limited image resolution in light microscopes, which is imposed by the wavelength of visible light. Only after electron microscopes were developed it

was realized that there are many other equally sound reasons for using electrons, most of which are utilized to some extent in a modern TEM.

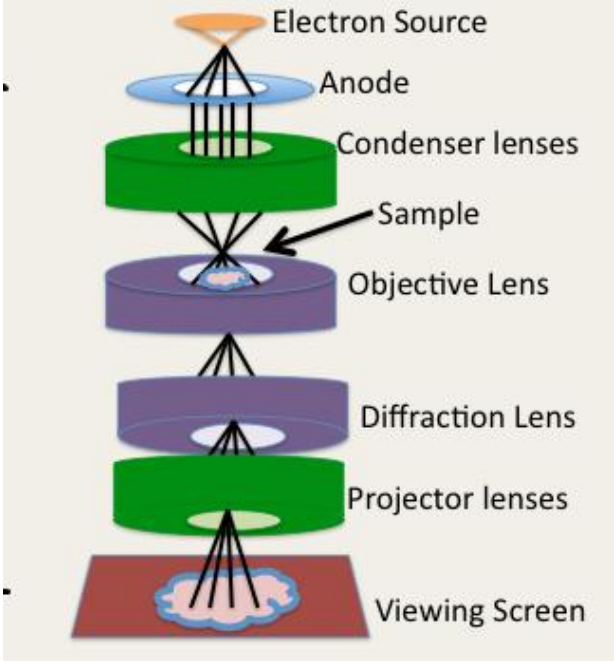

Fig. 3. 7: Main components of TEM

Principle

Transmission electron microscopy is a microscopy technique where by a beam of electron is transmitted through an ultra- thin specimen, interacting with the specimen as it passes through. An image is formed from the interaction of the electron transmitted through the specimen. The image is magnified and focused onto an imaging device, such as a fluorescent screen, on a layer of photographic film or to detect by a sensor such as a CCD camera. TEM are capable of imaging at a significantly higher resolution than light microscope, owing to small de Broglie wavelength of electrons

This enables the instrument's user to examine fine details even as small as a single column of atoms, which is tens of thousands times smaller than smallest resolvable object in the light microscope. TEM forms a major analysis method in a range of scientific fields, in both

physical and biological sciences. At higher magnifications complex wave interaction modulates the intensity of the image, requiring expert analysis of observed images. Alternate modes allow TEM to observe modulations in chemical identity, crystal orientation and morphology.

Instrumentation

A TEM is composed of several components as shown in fig. 3.7 which include:

1. A vacuum system in which the electrons travel, an electron emission source for generation of the electron stream.
2. A series of electromagnetic lenses, as well as electrostatic plates. These allow the operator to guide and manipulate the beam as required.
3. Device to allow the insertion into, motion within, and removal of specimens from the beam path.
4. Imaging devices are subsequently used to create an image from the electrons that exit the system.

Applications

The instrument allows performing the following analysis:

1. Morphological analysis.
2. Structural analysis by electron diffraction.
3. EDS qualitative and semi-quantitative analysis.

3.5.6 KD2 pro thermal properties analyzer

The KD2 Pro is device used to measure thermal properties of materials. The single- needle sensors measure thermal conductivity and resistivity; while the dual-needle sensor measures volumetric specific heat capacity and diffusivity. The KD2 Pro has been designed for ease of use and maximum functionality.

Principle of measurement

The KD2's sensor needle contains both a heating element and a thermistor. The thermal conductivity measurement makes several assumptions like: (i) the long heat source can be treated as an infinitely long heat source (ii) the medium is both homogeneous and isotropic, and at uniform initial temperature. Although these assumptions are not true in the strict sense, they are adequate for accurate thermal property measurements. The KS-1 sensor needle can be used for measuring thermal conductivity of fluids in the range of 0.2–2 W/m-K with accuracy of ±5%. Each measurement cycle consists of 90 s. During the first 30 s, the instrument will equilibrate which is then followed by heating and cooling of sensor needle for 30 s each. At the end of the reading, the controller computes the thermal conductivity using the change in temperature (ΔT)–time data.

Chapter 4 Results and Discussion

4.1 X-Ray Diffraction (XRD) analysis

Structural and phase analysis of SNPs and silica coated SNPs were carried out using PANalytical X'Pert Pro diffractometer operated at 45 kV and 40 mA at 25˚C with monochromatic Cu-Kα radiation (λ=1.5406Å). The XRD pattern of samples were recorded at 2θ (10 to 80 degree) with step size of 0.02 degree. The XRD patterns of as-synthesized SNPs and silica coated SNPs are shown in fig. 4.1. All the four peaks observed at 2θ: 38.26 (111), 44.42 (200), 64.55 (220), 77.58 (311) agrees well with the Joint Committee on Powder Diffraction Standards (JCPDS) card 01-087-0719, confirming the face centered cubic crystal of Ag nanoparticles. d-spacing and lattice parameter are calculated using equations:

$$\mathbf{n\,\lambda = 2\,d\,\sin\theta} \text{ and } \mathbf{1 / d^2 = (h^2+k^2+l^2) / a^2}$$

Where λ is the wavelength of incident X- rays (λ=1.5406 Å), d is spacing between planes, a is the lattice parameter, (h k l) corresponds to the miller indices of the planes and θ is Bragg's angle for diffraction. Calculated d-spacing and lattice parameter are shown in table 4.1. Average d-spacing and lattice parameters are 1.76 Å and 4.07 Å respectively. All the peaks in the XRD pattern are broaden irrespective of 2θ, which indicates that the broadening is due to nano size of silver particles.

The average crystallite size of silver nanoparticles and silica coated silver nanoparticle were calculated using Debye-Scherer's formula.

$$\mathbf{D = 0.9\times \lambda / \beta \cos\theta}$$

Where λ is the characteristic wavelength of radiation used for diffraction (λ =1.54016 Å), β is the full width at half maxima (FWHM) of highest intense peak (111). θ is Bragg's angle of diffraction. Calculated Crystallite size for SNPs and silica coated SNPs are 24.7 nm and 26.2 nm.

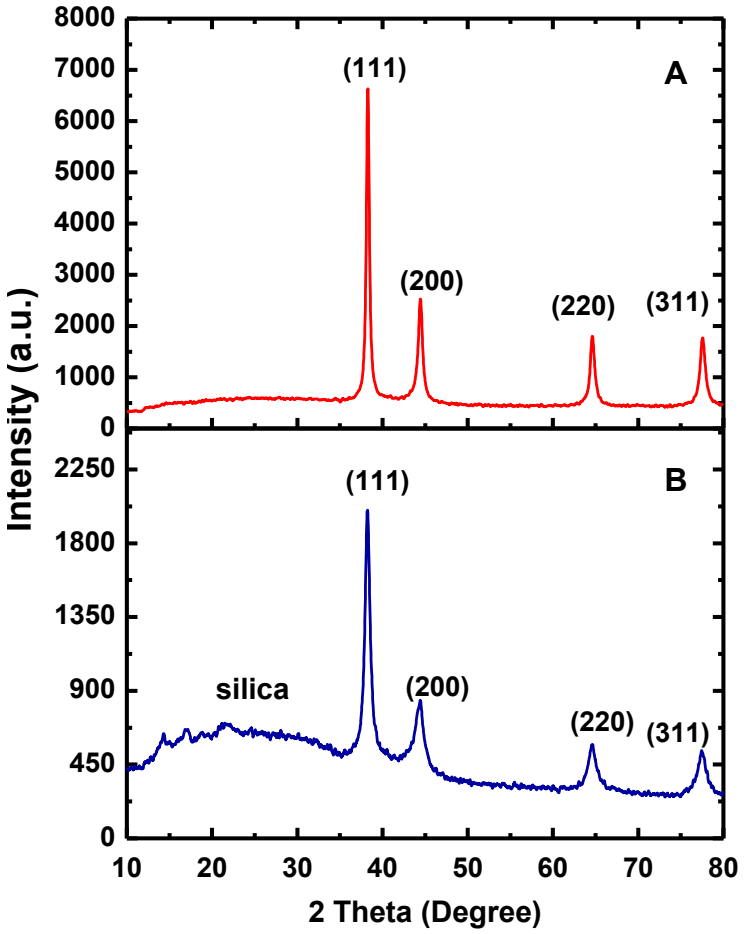

Fig. 4. 1: XRD Pattern of: (A) SNPs (B) Silica coated SNPs

Table 4. 1: d-spacing and lattice parameters for SNPs

Peak positions (2θ)	Corresponding planes	d-spacing (Å)	Lattice parameter (Å)
38.26	(111)	2.35	4.07
44.42	(200)	2.03	4.06
64.55	(220)	1.45	4.10
77.58	(311)	1.23	4.07

4.2 UV-Visible Spectral Analysis

The UV-Visible absorption spectra of silver nanoparticles (SNPs) and those coated with silica (SiO_2) were obtained on Hitachi made double beam spectrophotometer (U-3900H). The measurements were performed in quartz cuvettes at room temperature. Surface plasmon resonances (SPR) for SNPs and silica coated SNPs were observed. SPR for both types of nanoparticles centered at 409 nm in visible region of electromagnetic spectra as shown in fig. 4.2. These sharp peaks at 409 nm in both cases indicate that nanoparticles formed have spherical geometry in accordance with literature [50]. Before coating, the SNPs had a characteristic SPR peak at a wavelength of 409 nm. Although average particle diameter of silica coated Ag colloid were significantly increased from 17 to 27 nm, characteristics SPR peaks remained at around 409 nm. Peak position is not too sensitive to changes in coating thickness because the refractive index of silica is similar to that of water the plasmon peak remained at 409 nm [51].

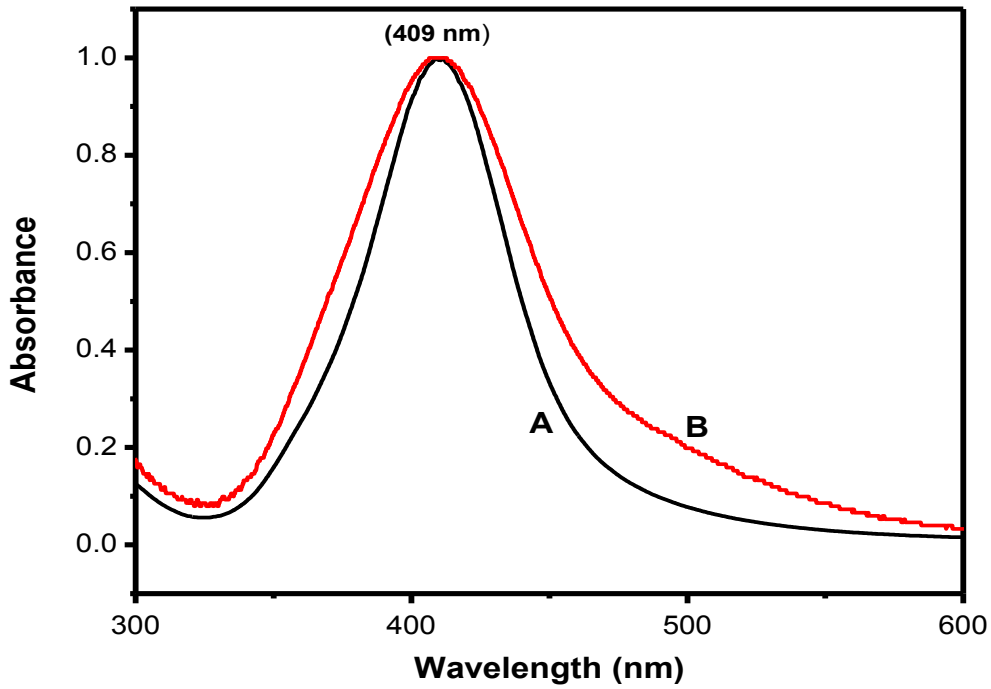

Fig. 4. 2: UV-Visible spectra of: (A) SNPs and (B) Silica coated SNPs

4.3 Dynamics light scattering (DLS) analysis:

The hydrodynamic size of SNPs and silica coated with SNPs is obtained on Brookhaven 90 plus particles size analyzer at room temperature. The hydrodynamic particle size is obtained by fitting with lognormal particle size distribution. The hydrodynamic size of SNPs and silica coated SNPs obtained are 24.76± 0.085 nm and 31.84± 0.10 nm respectively. This gives first hand confirmation that particles formed in this synthesis lies in nanometer size range which is further confirmed by transmission electron microscopy.

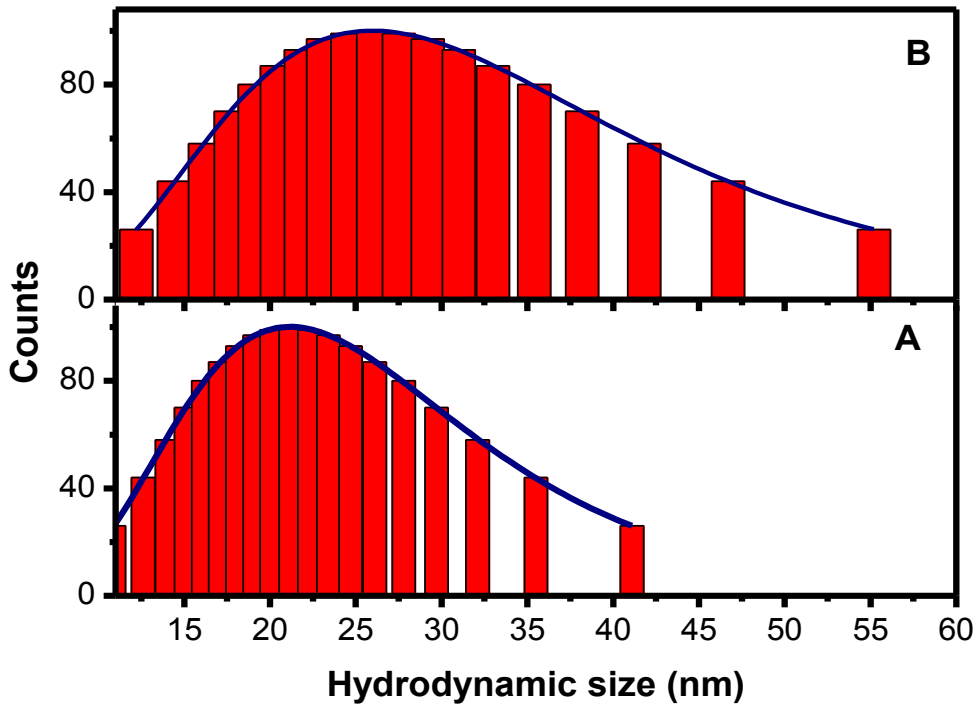

Fig. 4. 3: Represents hydrodynamic size distribution of (A) SNPs and (B) silica coated SNPs

4.4 Transmission electron microscopy analysis (TEM) analysis

Transmission electron microscopy is used to study the morphology of SNPs and silica coated SNPs. TEM micrographs were recorded on a Philips transmission electron microscope (CM200) operated at an accelerating voltage of 200 kV. Selected area electron diffraction (SAED) pattern were obtained on a JEOL (GEM 200) at 200 kV. Samples for TEM measurements are prepared

by placing a drop of colloidal dispersions of SNPs and silica coated SNPs in water on an amorphous carbon- coated copper grid. Fig. 4.4 shows that the both SNPs and SiO_2 coated SNPs have spherical morphology.

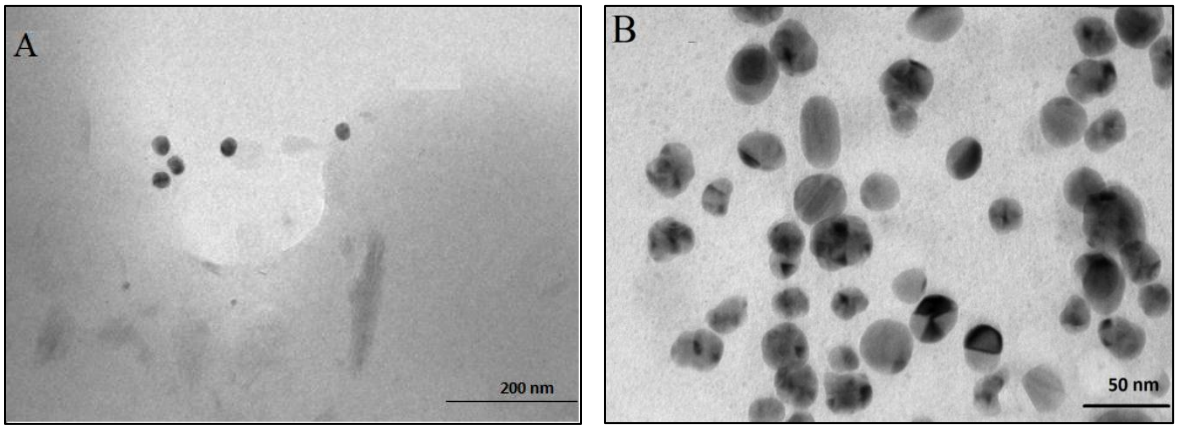

Fig. 4. 4: TEM images of: (A) SNPs (B) Silica coated SNPs

Average physical particle size of SNPs and silica coated SNPs are 17.67 nm and 27 nm respectively. Four distinguished rings appear in the selected area electron diffraction (SAED) pattern of SNPs as shown in fig. 4.5. These rings confirm the polycrystalline nature of nanoparticles. The d-spacing of these rings are in reasonably good agreement with that observed in X-ray diffraction analysis as shown in table 4.2

Table 4. 2: Planes corresponding to SAED of SNPs

d- spacing (JCPDS-Ref. no. 01-087-0719)	Observed d-spacing (TEM)	Observed d-spacing (XRD)	(h k l) index
2.35	2.29	2.35	(111)
2.03	1.98	2.03	(200)
1.43	1.42	1.45	(220)
1.22	1.19	1.23	(311)

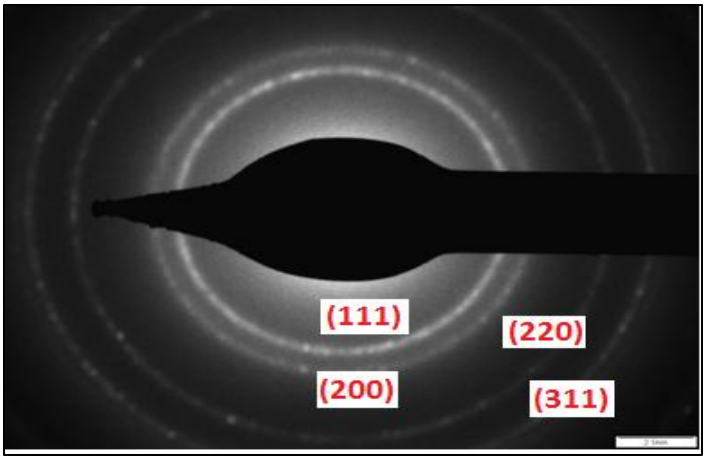

Fig. 4. 5: SAED pattern of as-synthesized SNPs

4.5 Fourier transformed infrared spectroscopy (FTIR) Analysis

FTIR spectra were recorded on a Perkin Elmer Spectrum BX (II) spectrophotometer in transmission mode for a liquid samples is shown in fig. 4.6. The characteristic bands observed are shown in table 4.3. Bands at 2928 and 2883 cm^{-1} corresponds to the asymmetric and symmetric stretching vibrations of $–CH_2-$ respectively. The bands at 3462 $cm^{-1}$is attributed to the stretching vibration absorption of (–OH-) of adsorbed water as PVP is hygroscopic

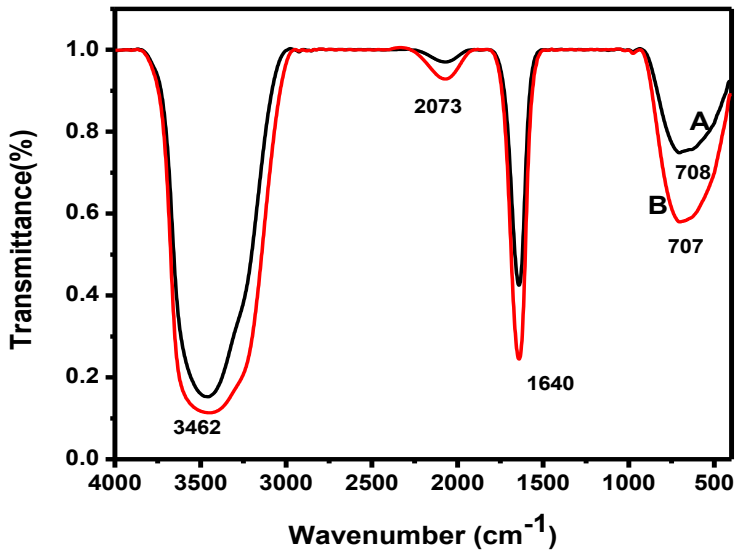

Fig. 4. 6: FTIR spectra of: (A) SNPs (B) silica coated SNPs

Table 4. 3 FTIR band positions for PVP and PVP capped SNPs

Bands position for PVP[52]	Observed Band positions for PVP capped SNPs
722	708
1080	1087
1118	1120
1289	1261
1661	1641
2885	2853
2951	2928
3431	3462

4.6 Thermal conductivity analysis

KD2 pro made by Decagon Devices was used to measure thermal conductivity of Ag/water and SiO_2 coated Ag/water nanofluids. This hand held device uses the transient line heat source technique to evaluate the fluid thermal properties. The instrument has 5 % accuracy over the 5^{o}C to 40^{o}C temperature.

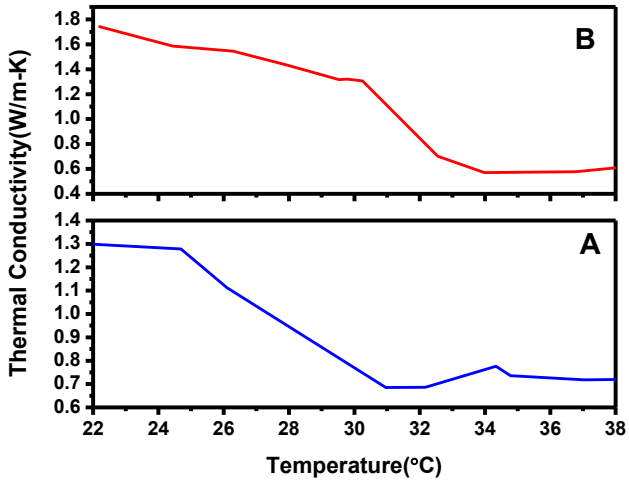

Fig. 4. 7: Thermal conductivity of: (A) SNPs based nanofluids (B) silica coated SNPs based nanofluids

First, thermal conductivity of Ag/water and SiO_2 coated Ag/water nanofluids were measured at room temperature and then variation in thermal conductivity with temperature (22-38°C) were plotted as shown in fig. 4.7.Both samples showed thermal conductivity decreases with increases in temperature then become independent of temperature in the range of 34-38° C**.**

Conclusion

- Silver nanofluid and silica coated silver nanofluid have been prepared by one-step method.
- The XRD study confirms the face centered cubic (FCC) structure of SNPs and broad hump confirms the coating of silica on the surface of SNPs. The average crystallite size for SNPs and silica coated SNPs obtained from the peak broadening was 24.7 nm and 26.2 nm respectively.
- FTIR study also confirms the adsorption PVP and silica on the surface of SNPs.
- A UV-Visible spectra shows a SPR peak centered around 409 nm which confirms the formation of SNPs.
- DLS study provides hydrodynamics size for SNPs (24.76± 0.085 nm) and silica coated SNPs (31.84± 0.10 nm). This study gives first hand confirmation that synthesized particles lies in nanometer size range.
- TEM study reveals that the nanoparticles are nearly spherical in shape. The average physical size for SNPs and silica coated SNPs is 17.67 nm and 27 nm respectively. SAED pattern confirmed the polycrystalline nature of prepared SNPs.
- Thermal conductivity measurements showed the decrease in thermal conductivity with increase in temperature for SNPs /water and silica coated SNPs/water nanofluids.

Scope for future work

- Firstly, further experimental and theoretical research is required to find the major factors influencing the performance of nanofluids. Up to now, there is a lack of agreement between experimental results from different groups so it is important to systematically identify these factors. The detailed and accurate structural characterizations of the suspensions may be the key to explain the discrepancy in the experimental data.
- Increase in viscosity by the use of nanofluids is an important drawback due to the associated increase in pumping power. The applications for nanofluids with low viscosity and high conductivity are promising. Enhancing the compatibility between nano materials and the base fluids through modifying the interface properties of two phases may be one of the solution routes.

- The shape of the additives in nanofluids is very important for the properties therefore the new nanofluid synthesis approaches with controllable microscope structure will be an interesting research work.
- Stability of the suspension is a crucial issue for both scientific research and practical applications. The stability of nanofluids, especially the long term stability, the stability in the practical conditions and the stability after thermal cycles should be evaluated.
- There is lack of investigation of the thermal performance of nanofluids at high temperatures, which may widen the possible application areas of nanofluids, like in high-temperature solar energy absorption and high-temperature energy storage. At the same time, high temperature may accelerate the degradation of the surfactants used as dispersants in nanofluids and may produce more heat.

References

[1] M. Chandrasekar and S. Suresh, Heat transfer engineering, vol. 30 (2011) 1136-1150.

[2] M**.** Chopkar, P. K. Das and I. Manna, Scripta Materialia, vol. 55 (2006) 549–552.

[3] C. H. Chon, K. D. Kihm, S. P. Lee and S.U.S. Choi, Applied Physics Letter, vol. 87 (2005) 153107-1– 153107-3.

[4] K. S. Hong, T. K. Hong and H. S. Yang, Applied Physics Letters, vol. 88 (2006) 031901-1– 031901-3.

[5] S. H. Kim, S. R. Choi and D. Kim, ASME Journal of Heat Transfer, vol.129 (2007) 298–307.

[6] H. Xie, J. Wang and T. Xi, Journal of Applied Physics, Vol.91 (2002) 4568-4572.

[7] P.K. Namburu, D.P. Kulkarni, D. Misra and D.K. Das, Experimental Thermal and Fluid Science, vol. 32 (2007) 397–402.

[8] S.K. Das, N. Putra, P. Thiesen and W. Roetzel, Journal of Heat Transfer, vol. 125 (2003) 567‑574.

[9] H. Patel, S. K. Das, T .Sundararajan, N. A. Sreekumaran, B. George and T. Pradeep, Applied Physics Letter, vol.83 (2003) 2931–2933.

[10] D. C. Venerus, M. S. Kabadi, S. Lee and P. Luna, Journal of Applied Physics, vol.100 (2006) 094310.

[11] W. Yu, D.M France, J. L. Routbort and S.U.S. Choi, Heat Transfer Engineering. Vol.29 (2008) 432-460.

[12] X. Wang, X. Xu and S. U. S. Choi, Journal of Thermophysics and Heat Transfer, vol.13 (1999) 474–480.

[13] C. Tzeng, C. W. Lin and K. D. Huang, Acta Mechanica, vol. 179 (2005) 11–23.

[14] J. Zhou, Z. Wu, Z. Zhang, W. Liu and Q. Xue, Tribology Letters, vol. 8 (2000) 213–218.

[15] C. Y Tsai, H. T Chien, P. P. Ding, B. Chan, T. Y. Luh and P. H. Chen, Materials Letters, vol. 58 (2004) 1461–1465.

[16] P. Jang and S. U. S. Choi, Applied Thermal Engineering, vol. 26 (2006) 2457–2463.

[17] S. Vafaei, T. Borca-Tasciuc, M. Z .Podowski, A. Purkayastha and G. Ramanath, and P. M. Ajayan, Nanotechnology, vol. 17 (2006) 2523–252.

[18] M. F. Demirbas, Energy Sources Part B, vol.1 (2006) 85–95.

[19] S. Wu, D. Zhu, X. Zhang and J. Huang, Energy and Fuels, vol. 24 (2010) 1894–1898.

[20] T. P. Otanicar, P. E. Phelan, R. S. Prasher, G. Rosengarten and R. A. Taylor, Journal of Renewable and Sustainable Energy, vol. 2 (2010) 1-13.

[21] X. Fan, H. Chen, Y. Ding, P. K. Plucinski and A. A. Lapkin, Green Chemistry, vol.10 (2008) 670–677.

[22] S.U.S. Choi and J.A Eastman, Developments and Applications of Non-Newtonian Flows, vol. 231 (1995) 99–105.

[23] S. Lee, S.U.S Choi, S. Li, J.A Eastman, Transactions of the ASME, Vol.12 (1999) 280-289.

[24] G. Carotenuto, Applied Organometallic Chemistry, vol.15 (2001) 344-351.

[25] P. Keblinsi, S.R Phillpot, S.U.S.Choi and J.A Eastman, International Journal of Heat and Mass Transfer, Vol. 45 (2002) 55-863.

[26] S.K. Das, N. Putra, P. Thiesen and W. Roetzel, Journal of Heat Transfer, vol. 125 (2003) 567‑574.

[27] H. Wang, X. Qiao, J. Chen and S. Ding, Colloids and Surfaces A: Physicochemical and Engineering Aspects, vol. 256 (2005) 111–115.

[28] T. Cho, I. Baek, J. Lee and S. Park, Journal of Industrial Engineering Chemistry, vol.11 (2005) 400-406.

[29] D. Kim, S. Jeong and J. Moon, Nanotechnology, vol.17 (2006) 4019-4024.

[30] J. S. Kim, Journal of Industrial Engineering. Chemistry, vol.13 (2007) 566-570.

[31] M.A.S. Sadjadi, B. Sadeghi, M. Meskinfam, K. Zare and J. Azizian, Physica E, vol. 40 (2008) 3183– 3186.

[32] S. G. Kim, N. Hagura, F. Iskandar and K. Okuyama, Advanced Powder Technology, vol. 20 (2009) 94-100.

[33] J. E. Milestone, S. J. Hurst, G.S. Metraux, J. I. Cutler and C. A. Mirkin, Small, vol.6 (2009) 646-664.

[34] H. A. Mintsa, G.Roy, C. T. Nguyen and D. Doucet, International Journal of Thermal Sciences, vol. 48 (2009) 363–37.

[35] M. Chandrasekara, S. Suresh and A. C. Bose, Experimental Thermal and Fluid Science, vol. 34 (2010) 210–216.

[36] J. G. Barrasa, J. M. Lopez-de-Luzuriage and M. Monge, Central European journal of chemistry, vol.9 (2011) 7-19.

[37] M. Chandrasekar and S. Suresh, Heat Transfer Engineering, vol. 30 (2011) 1136-1150.

[38] E. P. J. Sudhan and K. S. Meenakshi, Indian Journal of Science and Technology, Vol.4 (2011) 417-42.

[39] C. Pang, J. Y. Jung, J. W. Lee and Y. T. Kang, International Journal of Heat and Mass Transfer, vol.55 (2012) 5597–5602.

[40] R. S. Khedkar, S. S. Sonawane and K. L. Wasewar, International Communications in Heat and Mass Transfer, vol. 39 (2012) 665–669.

[41] Chandni, N. Andhariya, O.P. Pandey and B. Chudasama, Royal Society of Chemistry, vol.3 (2013) 1127-1136

[42] J. M. Salehi, M. M. Heyhat, and A. Rajabpour, Applied Physics Letters, vol.102 (2013) 231907(1-7).

[43] X. Fang, Q. Ding, L.W. Fan, Z. T. Yu, X. Xu, G.H. Cheng, Y.c. Hu and K.F. Cen, Journal of Heat Transfer , Vol. 136 (2014) 034501(1-7).

[44] W. Yu, D. M. France, J. L. Routbort and S. U. S. Choi, Review and Comparison of Nanofluid Thermal Conductivity and Heat Transfer Enhancements, Heat Transfer Engineering, vol. 29 (2008) 432–460.

[45] M. Chandrasekar and S. Suresh , Heat transfer engineering, vol. 30 (2011) 1136-1150.

[46] J. A. Eastman, S. U. S. Choi, S. Li, W. Yu and L. J. Thompson, Applied Physics Letters, vol. 78 (2001) 718–720.

[47] T.H. Zhu, Y. S. Lin and Y. S. Yin, Journal of Colloid and Interface Science, vol. 277 (2004) 100–103.

[48] J. S. Kim, Reduction of Silver Nitrate in Ethanol by Poly (N-vinylpyrrolidone), Journal of Industrial Engineering. Chemistry, vol.13 (2007) 566-570.

[49] G.J. Cho, B.M. Fung, D.T. Glatzhofer, J.S. Lee, Y.G. Shul, Langmuir, vol. 17 (2001) 456-461.

[50] S. G. Kim, N. Hagura, F. Iskandar and K. Okuyama, Advanced Powder Technology, vol. 20 (2009) 94-100.

[51] Y. Lu, Y. Yin, Z. Y .Li and Y. Xia, Nano letter, vol.2 (2002) 785-788.

[52] T. Zhaoa, R. Sun, S. Yu , Z. Zhang, L. Zhou, H. Huang, R. Du, Colloids and Surfaces A: Physicochemical and Engineering Aspects, vol. 366 (2010) 197–202.